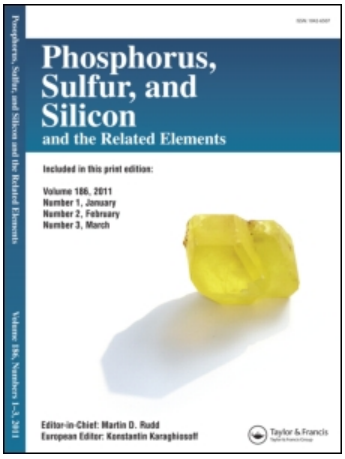

Phosphorus, Sulfur, and Silicon and the Related Elements
Publication details, including instructions for authors and subscription information:
http://www.informaworld.com/smpp/title~content=t713618290

Studies on the Chelation of Cyclodiphosph(V)azane Complexes of Co(II), Ni(II), Cu(II), and Pd(II): Preparation, Characterization, Thermal, Solid State Electrical Conductivity, and Biological Activity Studies

Abdel-Nasser M. A. Alaghaz[a]; Reda A. Ammar[b]; Hany M. Mohamed[a]
[a] Department of Chemistry, Faculty of Science, Al-Azhar University, Nasr City, Cairo, Egypt [b] Department of Chemistry, Faculty of Science, Al-Azhar University (Girls), Nasr City, Cairo, Egypt

To cite this Article Alaghaz, Abdel-Nasser M. A. , Ammar, Reda A. and Mohamed, Hany M.(2009) 'Studies on the Chelation of Cyclodiphosph(V)azane Complexes of Co(II), Ni(II), Cu(II), and Pd(II): Preparation, Characterization, Thermal, Solid State Electrical Conductivity, and Biological Activity Studies', Phosphorus, Sulfur, and Silicon and the Related Elements, 184: 9, 2472 — 2490
To link to this Article: DOI: 10.1080/10426500802505507
URL: http://dx.doi.org/10.1080/10426500802505507

Phosphorus, Sulfur, and Silicon, 184:2472–2490, 2009

ISSN: 1042-6507 print / 1563-5325 online
DOI: 10.1080/10426500802505507

Taylor & Francis
Taylor & Francis Group

Studies on the Chelation of Cyclodiphosph(V)azane Complexes of Co(II), Ni(II), Cu(II), and Pd(II): Preparation, Characterization, Thermal, Solid State Electrical Conductivity, and Biological Activity Studies

Abdel-Nasser M. A. Alaghaz,[1] Reda A. Ammar,[2] and Hany M. Mohamed[1]
[1]Department of Chemistry, Faculty of Science, Al-Azhar University, Nasr City, Cairo, Egypt
[2]Department of Chemistry, Faculty of Science, Al-Azhar University (Girls), Nasr City, Cairo, Egypt

Cyclodiphosph(V)azane of chromene, (1,3-diphenyl-2,4-bis(3-amino-9-methoxy-1-tolyl-3H-benzo[f]chromene-2-carbonitrile)-2,2,4,4-tetrachlorocyclodiphosph(V)-azane (III), reacts with stoichiometric amounts of transition metal salts such as Co(II), Ni(II), Cu(II), and Pd(II) to afford colored complexes in a moderate to high yield. The structure of the isolated complexes was suggested based on elemental analyses, IR, molar conductance, UV-Vis, ^{1}H, ^{13}C, and ^{31}P-NMR, magnetic susceptibility measurements, and dark electrical conductivity of solid state from room temperature up to 450 K. The complexes have been investigated in solution by spectrophotometric molar ratio and conductometric methods. Kinetic and thermodynamic parameters were computed from the thermal decomposition data using the Coats and Redfern method. The prepared complexes showed high to moderate bactericidal activity compared with the ligand.

Keywords Chromene; cyclodiphosph(V)azane; electrical conductivity; electronic; magnetic moment; ^{31}P NMR, IR

INTRODUCTION

The reaction of hexachlorocyclodiphosph(V)azanes with aromatic and aliphatic amines, active methylene-containing compounds, and bifunctional reagents and their metal complexes have been investigated.[1–6] In the present work, the interaction of hexachlorocyclodiphosph(V)azane (**I**) with aminochromene derivative and its metal complexes have been reported. The proposed structure for **III** is shown in Scheme 1.

Received 20 May 2008; accepted 25 September 2008.
Address correspondence to A. M. A. Alaghaz, Department of Chemistry, Faculty of Science (Boys), Al-Azhar University, Nasr City, Cairo, Egypt. E-mail: aalajhaz@hotmail.com

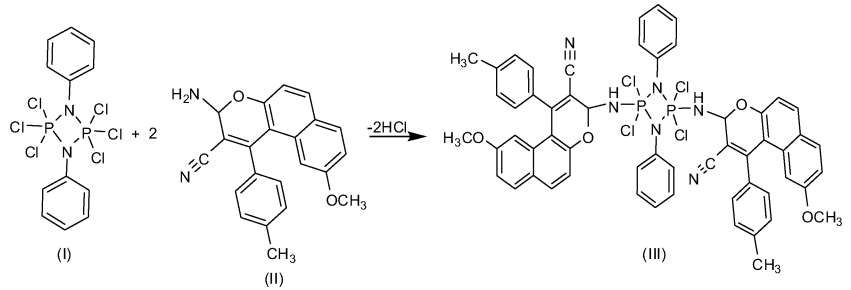

SCHEME 1 Structure of ligand III: 1,3-diphenyl-2,2,4,4-tetrachloro-2′,4′-bis(3-amino-9-methoxy-1-p-tolyl-3H-benzo[f]chromene-2-carbonitrile) cyclodiphosph(V)azane.

RESULTS AND DISCUSSION

A new aminocyclodiphosph(V)azane-based ligand (III) was synthesized by the reaction between 1,3-diphenyl-2,2,2,4,4,4-hexachlorocyclodiphosph(V)azane (**I**) and 3-amino-9-methoxy-1-phenyl-3H-benzo[f]chromene-2-carbonitrile as shown in Scheme 1. The ligand was found to be soluble in $CHCl_3$, acetone, ethanol, THF, methanol, DMSO, DMF, acetone, and ethyl acetate and insoluble in diethyl ether and water, slightly soluble in benzene and *n*-hexane. The structure of the ligand (**III**) was elucidated by elemental analyses (Table I), IR, electronic, ^1H, ^{13}C, and ^{31}P NMR techniques.

IR Spectra

The assignments of the important bands of the free ligand are given in Table II. The spectra reveal the characteristic bands of the ν_{P-NH} stretching vibrations of the ligand at 2620 cm^{-1}, which is similar to those assigned by Abd-Ellah[7] and Pustinger.[8] The band that appeared at 3153 cm^{-1} is attributed to the ν_{NH} stretching vibration. The band observed at 2218 cm^{-1} is ascribed to the $\nu C{\equiv}N$ stretching vibration that appeared at 2182 cm^{-1} in compound (**II**). The shift of this band to higher frequency in the ligand is considered as evidence for the ligand formation. The band at 1226 cm^{-1} was assigned to the ν_{P-N} stretching vibration.[9–12] The ν_{P-Cl} stretching vibration is observed at 490 cm^{-1}.[13] Bands appearing in the range 1622–1409 cm^{-1} may be attributed to $\nu_{C=C}$.[13] Moreover, the IR spectra showed a weak band at 879 cm^{-1} due to the ν_{C-O} stretching vibration of chromene ring.[14] The weak band observed at 2929 cm^{-1} is due to aromatic C—H stretching vibrations.[15]

TABLE I Elemental Analyses, Yields, Colors, and Melting Points of Ligand (III) and Its Corresponding Metal Complexes (IVa–d)

Compd. no. M.F. (M. wt)	mp (°C) [Color]	Yield (%)	Elemental analyses found (Calcd), %						Λ^a
			C	H	N	P	Cl	M	
III $C_{54}H_{40}Cl_4N_6O_4P_2$ (1040.69)	198 [Yellow]	90.2	62.36 (62.32)	3.17 (3.87)	8.13 (8.08)	5.90 (5.95)	13.43 (13.63)	—	
IV$_a$ $C_{54}H_{40}Cl_8Co_2N_6O_4P_2$ (1300.37)	>360 [Green]	92.8	49.45 (49.88)	3.00 (3.10)	6.44 (6.46)	4.70 (4.76)	21.42 (21.81)	9.00 (9.06)	7.85
IV$_b$ $C_{54}H_{40}Cl_8N_6Ni_2O_4P_2$ (1299.89)	>360 [Brown]	92.7	49.10 (49.89)	3.13 (3.10)	6.33 (6.47)	4.70 (4.77)	21.46 (21.82)	9.00 (9.03)	11.39
IV$_c$ $C_{54}H_{40}Cl_8Cu_2N_6O_4P_2$ (1309.60)	>360 [Brown]	97.6	49.48 (49.53)	32.11 (3.08)	6.24 (6.42)	4.51 (4.73)	21.54 (21.66)	9.70 (9.70)	18.30
IV$_d$ $C_{54}H_{40}Cl_4N_{10}O_{16}P_2Pd_2$ (1501.5)	>360 [Brown]	97.6	43.11 (43.19)	2.61 (2.69)	9.21 (9.33)	4.10 (4.13)	9.39 (9.44)	—	18.30

$^a(\Omega^{-1}\ mol^{-1}\ cm^2)$.

TABLE II Characteristic IR Stretching Vibration Bands (cm^{-1})[a] of the Ligand (III) and Its Metal Complexes (IV_{a-d})

Compd. no.	$\nu_{(NH)}$	$\nu_{(M-Cl)}$	$\nu_{(P-N)}$	$\nu_{(P-N)}$	$\nu_{(M-N)}$	$\nu_{(P-NH)}$	$\nu_{(C\equiv N)}$
III	3153 br	—	490 m	1226 m	—	2620 m	2218 v.s
$\mathbf{IV}_a$	3126 br	250 m	488 m	1186 m	667 w	2619 m	2203 m
$\mathbf{IV}_b$	3125 br	297 w	488 m	1198 m	685 m	2620 m	2203 s
$\mathbf{IV}_c$	3128 br	300 w	484 m	1187 m	694 m	2620 m	2206 m
$\mathbf{IV}_d$	3123 br	298 w	492 m	1196 m	684 m	2620 m	2200 m

[a] v.s = very strong, s = strong, m = medium, w = weak, br = broad.

Electronic Spectra

The fact that the expected band at 275 nm,[16] characteristic for the delocalization of the nonbonding electrons on the nitrogen atoms within the phosphazo ring of the dimeric structure was observed in the spectrum of ligand (**III**), suggested the presence of the phosphazo ring. The bathochromically shifted band observed at 287 nm for the ligand relative to that of the dimer (**I**) is explained to be due to the replacement for one chlorine atom of each phosphorus atom by the 1,3-diphenyl-2,4-bis(3-amino-9-methoxy-1-phenyl-3H-benzo[f]chromene-2-carbonitrile. The new band observed at 350 nm is attributed to the n-π^* transition of attached compound (**II**), which is absent in the corresponding dimer (**I**) and this is considered evidence for the ligand formation.

Metal Complexes

The chemical behavior of **III** toward transition-metal cations was our goal in this article. The metal cations selected for this purpose were Co(II), Ni(II), Cu(II), and Pd(II). When a mixture of one mole of **III** in acetonitrile was reacted with two moles of the metal salts in acetonitrile, a change in color was observed and the complex compounds precipitated. The products were purified by washing with acetonitrile and gave elemental analysis compatible with the general formula $[(MX_2)_2(\mathbf{III})]$, where M = Co(II) (X = Cl), Ni(II) (X = Cl), Cu(II) (X = Cl), and Pd(II) ($X = NO_3$). Accordingly, the complexes are prepared following the general equation:

$$2MX_2 + \mathbf{III} + mH_2O \rightarrow [(MX_2)_2(\mathbf{III})]$$

where M = Co(II) (X = Cl, m = 0), Ni(II) (X = Cl, m = 4), Cu(II) (X = Cl, m = 0), and Pd(II) ($X = NO_3$, m = 0).

The analytical data of the isolated complexes are listed in Table I. The complexes was found to be soluble in DMSO, DMF, and THF and insoluble in $CHCl_3$, ethanol, diethyl ether, and water, slightly soluble in acetone. Further, the proposed structures of the complexes of **III** is confirmed using different physicochemical tools such as IR, molar conductance, UV-Vis, solid reflectance, magnetic moment, and solid-state electrical conductivity.

IR Spectra

The most important vibrational bands of the ligand and its metal complexes are given in Table II. The results of IR spectra of the metal complexes show absorption bands of both $\nu_{C\equiv N}$ and ν_{N-H} at lower frequencies than those of the free ligand **III**, indicating that the metal ions are coordinated to the nitrogen atoms of both C≡N and N–H groups of the ligand **III**. Further, in all the metal complexes, there were new medium to weak bands observed at lower frequencies in the range (250–300 cm^{-1}) that were assigned to ν_{M-N}.[13]

The ν(M-Cl) band is observed at 340–348 cm^{-1} and 308–312 cm^{-1}, which showed terminal rather than bridging chlorine for the chloro complexes.[17]

The nitrato complex, having two bands at 1280 cm^{-1} and 1390 cm^{-1} corresponding to ν_1 and ν_4 of the nitrato groups with a separation Δ of 110 cm^{-1}, points toward monodentate coordination.[17,18] The appearance of a band at 1390 cm^{-1} in the spectrum of the complex that does not contain ionic nitrates is most probably due to the fact that a certain amount of coordinated nitrates transforms to ionic nitrates by pressing KBr pellet.[18] In addition, a weak band at 710 cm^{-1} assignable to the ν_3 mode is further support for the presence of a terminally bonded nitrato group.[13] This has been confirmed by the band at 362 cm^{-1}, which pointed to the coordination of the nitrate group through oxygen.[18]

The characteristic bands corresponding to the ν_{P-NH}, ν_{P-N}, and ν_{NH} associated with all the investigated complexes are collected in Table II.

Spectrophotometric Measurements of Solution Stoichiometry

The absorption values of the Cu^{2+} complexes are shown in Table III. The diagrams in Figure 1 consist of two linear portions intersecting at 1:2 [ligand]/[Cu^{2+}], indicating the formation of 2Cu(II):IL species.[19] This is in agreement with the elemental analyses and conductometric analyses data.

TABLE III Absorption Data of Ligand (III) Solution with the Addition of Cu^{2+}Solution, (IV_c)

Molar ratio (Cu^{+2}: III)	Conc. of III (10^{-4}M)	Conc. of Cu (10^{-4}M)	Absorbance
0	0	2.0	0.157
2:0.25	0.25	2.0	0.164
2:0.50	0.50	2.0	0.171
2:0.75	0.75	2.0	0.172
2:1.00	1.0	2.0	0.181
2:1.25	1.25	2.0	0.183
2:1. 50	1.50	2.0	0183
2:1.75	1.75	2.0	0.183
2:2.00	2.0	2.0	0.183
2:2.25	2.25	2.0	0.183
2:2.50	2.50	2.0	0.183
2:0.75	2.75	2.0	0.183
2:3.00	3.0	2.0	0.183

Conductometric Titration

In order to follow up the behavior of the ligand in solution with Co(II), Ni(II), and Cu(II), we investigated these systems using a conductometric titration method.[21] In this method, 25 mL (10^{-4} M) of M(II) where M(II) is Co(II), Ni(II), Cu(II), and Pd(II) solution in absolute ethanol was titrated with (10^{-3} M) of ligand solution absolute ethanol at room temperature 25°C and represented in Figure 2. The curves were plotted between the conductance of the solution and the volume of ligand added. The results show that the break in the curve occurred when the 2:1 (M:L) species are formed in solution. The conductance of

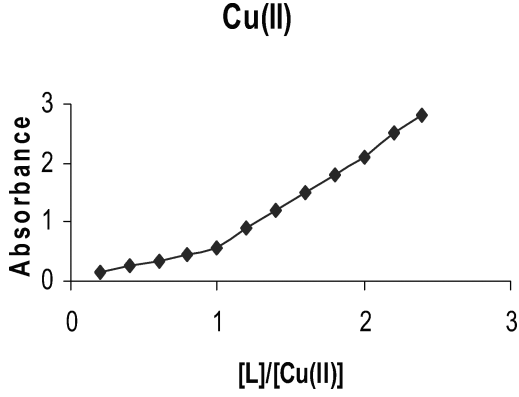

FIGURE 1 Results of molar ratio method for Cu(II) complex.

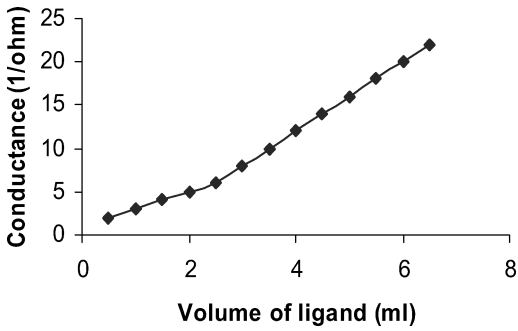

FIGURE 2 Conductometric titrations for Cu(II) complex.

the reaction mixture was increase continuously with complexes under investigation. The reason for increase in conductivity after 2:1 (M:L) complexes forms may be due to the presence of the ligand in ionic form in the medium (ethanol), which raises the conductivity.[19]

Molar Conductance Data

The molar conductance values in DMF at 25°C (Table I) for the complexes were found to be in the range 7.85–18.30 Ω^{-1} mol^{-1} cm^2. The relatively low values indicate the nonelectrolytic nature of these complexes. It also indicates the nonbonding of the chloride or nitrate anions to the metal ions.

Electronic Spectra and Magnetic Properties

The electronic spectra of the free ligand exhibit bands at 345 and 285 nm, which could be assigned to n-π^* and π–π^* transitions, respectively. On complexation, the lower-energy band is shifted to a red shift, whereas the transition π–π^* is slightly shifted to a blue shift.

The room-temperature magnetic susceptibility measurement of the Co(II) complex, [Co_2(III) Cl_4] **IV**$_a$, gave magnetic moment value μ_{eff} of 3.54 B.M., corresponding to three unpaired electrons, which are expected for a weak field ligand. The electronic spectra of the Co(II) complex as nujol mulls and/or solution in ethanol were recorded in the range 280–900 nm. The spectra exhibit peaks at the 715 nm region, which may be assigned to $^4A_2 \rightarrow {}^4T_1$ (p) (ν_3) and is consistent with the tetrahedral geometry.[19] The peaks observed at the 295 nm and 248 nm regions were assigned to n-π^* and π–π^* transitions, respectively.[19]

The green Ni-complex, [Ni_2(III)Cl_4] **IV**$_b$, gives a value μ_{eff} of 2.91 B.M., which is indicative of two unpaired electrons. The electronic spectra of the Ni(II) complex **IV**$_b$ exhibit an absorption band near 665 nm,

which may be attributable to the $^3T_1 \rightarrow {}^3T_1$ (p), and weak bands observed on the high and low energy sides of the 660 nm band have been assigned to spin-forbidden bands.[19]

The Cu(II) complex, $[Cu_2(III)\ Cl_4]$ **IV**$_c$, absorbed at 698 nm was assigned to $^2B_2 \rightarrow {}^2E$ transition. The bands observed in the range 425 nm were assigned to the charge transfer via L → M (Cu^{2+}).[19] The observed band at 280 nm was attributable to π-π^*. The magnetic moment of the Cu(II)-complex of μ_{eff} value of 2.01 B.M. is in accordance with one unpaired electron, which is indicative of square planar structure.

Palladium complex has three spin allowed singlet–singlet d–d transitions, which are $^1A_1g \rightarrow {}^1A_2g$ (715 nm), $^1A_1g \rightarrow {}^1B_1g$ (495 nm), and $^1A_1g \rightarrow {}^1Eg$ (415 nm).[20] These transitions are from the lower lying d-orbital to the empty d_{x2-y2} orbital. The strong band at 375 nm is assignable to a combination of M → L (charge transfer) and d–d bands.

Solid State Electrical Conductivity

Figure 3 shows the relation between log σ against $1/T$ for 1,3-diphenyl-2,4-bis(3-amino-9-methoxy-1-phenyl-3H-benzo[f]-chromene-2-carboni-trile)-2,2,4,4-tetrachlorocyclodiphosph(V)azane compound and its complexes. A linear behavior was obtained for all samples. The conductivity of the free ligand is increased on complexing with transition metal ions. This behavior is attributed to the inclusion of the various metal cations in the π-electron delocalization of the ligand.[21] The observed conductivities follow the order Co < Ni < Cu. Theoretically, if we consider the charge/radii, the stability of the metal complexes increases as the size of the metal ion decreases or the value of the ratio charge/radii increases. This means that the stability increases toward the copper complex. It is apparent that increasing stability of the complexes will increase the number of dislocated electrons on the ligand molecule and then increase the conductivity[22] as given in Table IV. To explain the conduction mechanism of the ligand and its complexes, it is necessary to determine the mobility of charge carriers μ. If the density of charge carriers is known, then the mobility can be calculated using the relation $\sigma = eN\text{m}$, where e is the electron charge. The charge carrier concentration was determined using the relation

$$n = 2[2\ \mu m^* kT/h^2]^{1/2} \exp(-E/kT)$$

where m^* is the effective mass of charge carrier. The calculated mobilities range from 10^{-5} to 10^{-9} cm^2/Vs, suggesting that the conduction of

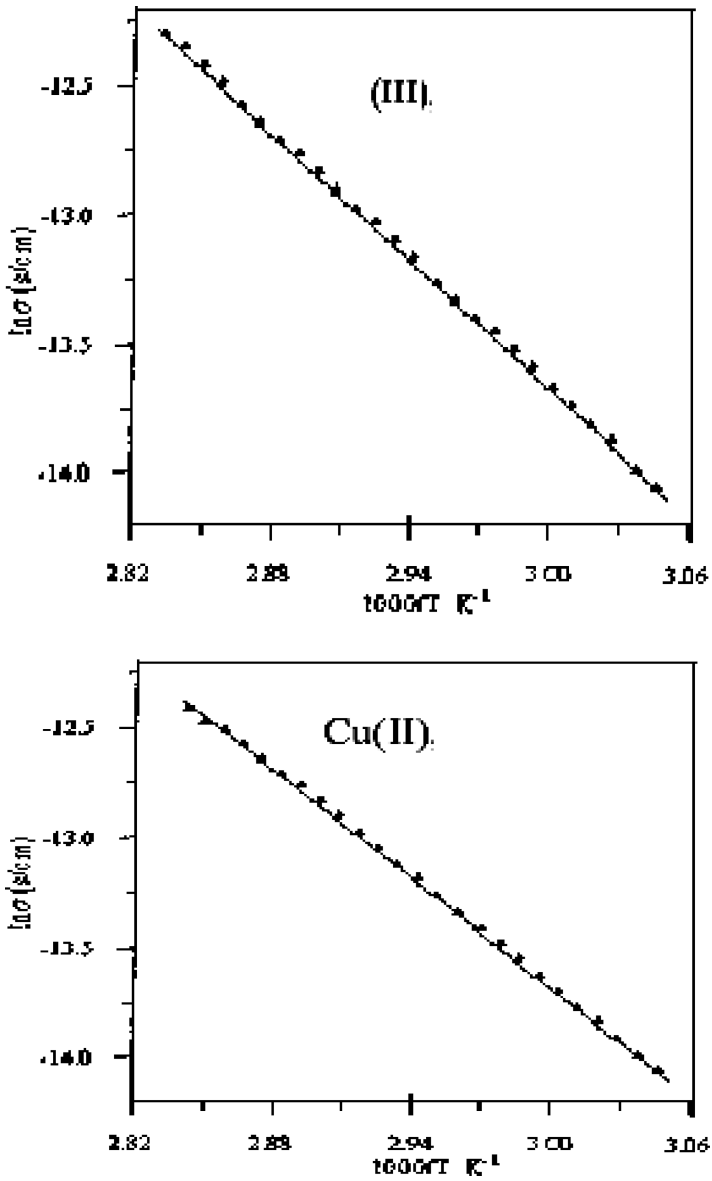

FIGURE 3 Plots of ln σ versus 1×10^{-3}/T for the ligand (III) and its $Cu^{2+}(IV_c)$ complex.

TABLE IV Values of the Electrical Conductivity (σ) and Thermal Activation Energy of the Ligand (III) and Its Complexes ($\mathbf{IV}_{a-d}$) at 303 K

Compound	$\sigma(\text{Ohm}^{-1}\text{cm}^{-1})$	E(eV)	$n(\text{cm}^{-3})$	$\mu(\text{cm}^2/\text{V s})$
III	1.50×10^{-8}	0.33	8.63×10^{19}	1.11×10^{-7}
$\mathbf{IV}_a$	1.8×10^{-8}	0.36	12.82×10^{18}	8.25×0^{-9}
$\mathbf{IV}_b$	2.12×10^{-8}	0.45	1.83×10^{18}	7.83×10^{-8}
$\mathbf{IV}_c$	2.64×10^{-8}	0.61	1.30×10^{16}	1.37×10^{-5}
$\mathbf{IV}_d$	2.83×10^{-8}	0.68	1.11×10^{16}	1.26×10^{-4}

chromene-cyclodiphosph(V)azane ligand and its metal complexes takes place by hopping mechanism.[23]

X-Ray Diffraction Characterization

Unit cell parameters were found by using trial and error methods as follows: the sample Co is monoclinic with the unit cell parameters a = 4.934 Å, b = 4.122 Å, c = 13.03 Å, $\beta = 98.64^\circ$, and cell volume V = 239.30 3 Å^3. Diffraction data, i.e., 2θ (observed), $\Delta 2\theta$, and indices of the N-Co sample, are calculated using these unit cell parameters.[24]

The N-Ni sample is tetragonal with the cell parameters a = 6.721 Å, c = 9.653 Å, c/a = 1.4211, and cell volume V = 427.598 Å^3. The N-Cu sample is triclinic with the cell parameters[24] a = 8.300 Å, b = 7.910 Å, c = 6.7455 Å, $\alpha = 100.09^\circ$, $\beta = 130.13^\circ$, $\gamma = 113.02^\circ$, and cell volume V = 290.553 Å.^{3}

ESR Spectrum of Cu(II) Complex

X-band ESR spectrum of the Cu(II) ($\mathbf{IV}_c$) complex was recorded in the solid state at 25°C. The spectrum exhibits one broad band with g = 2.01 for complex ($\mathbf{IV}_c$). The shape of the spectrum is consistent with the square planar geometry around the Cu(II) environment in the complex ($\mathbf{IV}_c$).[25]

Kinetics of Thermal Decomposition

Recently, there has been increasing interest in determining the rate-dependent parameters of solid-state nonisothermal decomposition reactions by analysis of TG curves.[26] Thermogravimetric (TG) and differential thermogravimetric (DTG) analyses were carried out for Co(II), Ni(II), Cu(II), and Pd(II)–III complexes in ambient conditions. The correlations between the different decomposition steps of the complexes

with the corresponding weight losses are discussed in terms of the proposed formula of the complexes.

The thermal decomposition of [Co(III)] complex(**IV**$_a$) with the molecular formula ($C_{54}H_{40}Cl_8Co_2N_6O_4P_2$ [M. wt. = 1300.37]) proceeds with two main degradation steps. The first step occurs within the temperature range 485–590 K with an estimated mass loss of 51.15% (calculated mass loss = 51.35%), which reasonably accounts for the loss of $C_{30}H_{27}N_4PCl_5O$ fragment. The DTG curve gives an exothermic peak at 638 K (the maximum peak temperature). The second step occurs within the temperature range 595–795 K with an estimated mass loss 36.73% (calculated mass loss = 36.99%), which reasonably accounts for the loss of rest of the ligand molecule, leaving 2CoO as residue. The DTG curve gives an exothermic peak at 705 K (the maximum peak temperature). Total estimated mass loss is 87.88% (calculated mass loss = 88.34%).

The thermal decomposition of [Ni(III)] complex (**IV**$_b$) with the molecular formula [$C_{54}H_{40}Cl_8N_6Ni_2O_4P_2$(M.wt. = 1299.89)] also proceeds with two main degradation steps. The first estimated mass loss of 51.23% (calculated mass loss = 51.37%) within the temperature range 592–625 K could be attributed to the liberation of $C_{30}H_{27}N_4PCl_5O$ fragment. The DTG curve gives an exothermic peak at 596 K (the maximum peak temperature). The second step occurs within the temperature range 650–815 K with an estimated mass loss 37.17% (calculated mass loss = 37.13%), which reasonably accounts for the decomposition of remaining part of the ligand molecule ($C_{24}H_{13}N_2PCl_3O$) leaving 2NiO as residue. The DTG curve gives an exothermic peak at 760 K (the maximum peak temperature). Total estimated mass loss is 88.40% (calculated mass loss = 88.50).

The complex [Cu(III)] (**IV**$_c$) with the molecular formula [$C_{54}H_{40}Cl_8Cu_2$-$N_6O_4P_2$(M. wt = 1309.60)] is thermally decomposed in two successive decomposition steps. The first estimated mass loss of 43.60% (calculated mass loss = 43.58%) within the temperature range 540–590 K may be attributed to the loss of ($C_{27}H_{20}N_3P_2Cl_3O$) fragment. The DTG curve gives an exothermic peak at 553 K (the maximum peak temperature). The second step occurs within the temperature range 661–853 K with the estimated mass loss 44.23% (calculated mass loss = 44.26%), which corresponds to the loss of $C_{27}H_{20}N_3Cl_5O$ fragment, leaving 2CuO as residue. The DTG curve gives an exothermic peak at 770 K (the maximum peak temperature). Total estimated mass loss is 87.83% (calculated mass loss = 87.84%).

The [Pd(III)] complex (**IVd**) with the molecular formula ($C_{54}H_{40}Cl_4$-$N_{10}O_{16}P_2Pd_2$ [M. wt. = 1501.5]) is thermally decomposed in two successive steps. The first estimated mass loss 58.73% (calculated mass

loss = 58.78%) within the temperature range 558–579 K can be attributed to the loss of ($C_{45}H_{28}Cl_2PN_6O_8$) fragment. The DTG curve gives an exothermic peak at 568 K (the maximum peak temperature). The second step occurs within the temperature range 593–698 K with an estimated mass loss 24.87% (calculated mass loss = 24.91%), which reasonably accounts for the loss of rest of the ligand molecule ($C_9H_{12}N_4Cl_2PO_6$), leaving 2PdO as residue with total estimated mass loss of 83.60% (calculated mass loss = 83.69%). The DTG curve gives an exothermic peak at 659 K (the maximum peak temperature).

The final product of decomposition at 875 K corresponds to the formation of metal oxide as the end product, which was confirmed by comparing the observed/estimated and the calculated mass of the pyrolysis product.

The kinetic analysis parameters such as activation energy (ΔE^*), enthalpy of activation (ΔH^*), entropy of activation (ΔS^*), and free energy change of decomposition (ΔG^*) were evaluated graphically by employing the Coats–Redfern relation:[27]

$$\mathrm{Log}[-(\log(1-\alpha)/\mathrm{T}^2)] = \log[\mathrm{AR}/\theta\mathrm{E}^*(1-2\mathrm{RT}/\mathrm{E}^*)] - \mathrm{E}^*/2.303\mathrm{RT} \quad (1)$$

where α is the mass loss up to the temperature T, R the gas constant, E^* is the activation energy in J mol^{-1}, θ is the linear heating rate, and the term $(1 - 2RT/E^*) \cong 1$. A straight line plot of left-hand side of Eq. 1 against $1/T$ gives the value of E^* , whereas its intercept corresponds to A (Arrhenius constant). The calculation of heat of reaction (ΔH^*; Table V) from the DTA curves was done by using the relation:

$$\Delta H^* = \Delta H(\mathrm{muv})60 \times 10^{-6}(\mathrm{MJmol}^{-1}) \quad (2)$$

TABLE V Thermodynamic Activation Parameters of Metal Complexes

No.	Order (n)	Steps	E^* (J mol^{-1})	A ($\times 10^5$s^{-1})	ΔS^* (JK^{-1}mol^{-1})	ΔH^* (J mol^{-1})	ΔG^* (kJ mol^{-1})
1	1	I	21.18	0.27	−163.14	186.93	103.15
		II	23.22	0.26	−157.37	1253.91	131.92
2	1	I	44.37	0.27	−164.43	92.85	89.93
		II	46.02	0.18	−158.54	2000.14	122.21
3	1	I	45.83	0.19	−157.13	263.38	98.94
		II	46.86	0.20	−158.36	2658.23	115.37
4	1	I	45.82	0.22	−159.60	272.79	97.76
		II	46.75	0.20	−158.55	2902.64	109.06

where M is the molar mass of the complex and muv = micro unit volt. The entropy of activation (ΔS^*) and the free energy change of activation (ΔG^*) were calculated using Eqs. 2 and 3:

$$\Delta S^* = 2.303R[\log(Ah/kT)](\mathrm{JK}^{-1}\ \mathrm{mol}^{-1}) \quad (3)$$

$$\Delta G^* = \Delta H^* - T\Delta S^*(\mathrm{J\ mol}^{-1}) \quad (4)$$

where k and h are the Boltzman and Plank constants, respectively. The calculated values of E^*, A, ΔS^*, ΔH^*, and ΔG^* for the decomposition steps of the complexes are appended in Table V. According to the kinetic data obtained from the TG curves, all the complexes have negative entropy, which indicates that the complexes are formed spontaneously. The negative value of entropy also indicates a more ordered activated state that may be possible through the chemisorption of oxygen and other decomposition products. The negative values of the entropies of activation are compensated for by the values of the enthalpies of activation, leading to almost the same values for the free energy of activation.[28]

Biological Activity

The disc diffusion method was used to measure the antimicrobial activity of the complexes.[29,30] The compounds under test were dissolved in dimethylformamide (DMF; 2% w/v) and added at a concentration of 0.5 mL/disc to Whatman number 3 filter paper, 5 mm diameter. The biological activity of **III**, its complexes, and traivid and tavinic (as standard compounds) were tested against bacteria because bacteriua can achieve resistance to antibiotics through biochemical and morphological modifications.[31] The antimicrobial activity was examined with different species of gram-positive bacteria such as *Staphylococcus pyogenes*, gram-negative bacteria such as *Pseudomonas aeruginosa* and *Escherichia coli*, and fungi (*Candida*). The data obtained are summarized in Table VI. The data obtained reflect the following findings:

1) The **III** ligand has moderate activity in comparison with *Staphylococcus pyogenes* and is less active in comparison with *Escherichia coli* and *Pseudomonas aeruginosa*. The remarkable activity of the ligand may arise from the imino-NH and carbonitrile-C≡N groups, which may play an important role in the antibacterial activity.[31]
2) Antibacterial activity of the complexes toward the different organisms shows high to moderate activity.
3) The activity of the ligand and its complexes increases as the concentration increases because it is a well-known fact that concentration plays a vital role in increasing the degree of inhibition.[32]

TABLE VI Antimicrobial Activity of III and Corresponding Metal Complexes

Compound	(mg/mL)	S. P.	P.A.	Fungus (*Candida*)	E.C.
III	5	+++	++	−	++
	2.5	++	++	−	+
	1	++	−	−	+
IV$_a$	5	+++	++	+	+++
	2.5	+	++	−	++
	1	+	+	−	+
IV$_b$	5	+++	++	+	++
	2.5	+++	++	−	++
	1	++	+	−	+
IV$_c$	5	++	++	+	++
	2.5	++	+	−	++
	1	++	+	−	+
IV$_d$	5	+++	++	+	++
	2.5	++	+	−	++
	1	+	+	−	+
Tavenic[a]	5	+++	+++	+	+++
	2.5	++	++	−	++
	1	+	+	−	+
Traivid[a]	5	++	++	−	++
	2.5	+	+	−	+++
	1	−	−	−	−

[a]Standard materials. Inhibition value = 0.1–0.5 cm beyond control = +; Inhibition value = 0.6–1.0 cm beyond control = ++; Inhibition value = 1.1–1.5 cm beyond control = +++; S.P. = *Staphylococcus pyogenes*; E.S. = *Escherichia coli*; and P.A. = *Pseudomonas aeruginosa*.

Structural Interpretation

From all of the above observations, the new ligand 1,3-diphenyl-2,4-bis(3-amino-9-methoxy-1-phenyl-3H-benzo[f]chromene-2-carbonitrile)-2,2,4,4-tetrachlorocyclodiphosph(V)azane (**III**) forms (2M:1L) complexes with the Co(II), Ni(II) Cu(II), and Pd(II) metal cations. The structural information from these complexes is in agreement with the data reported in this article based on the IR, molar conductance, UV-Vis, mass, solid reflectance, solid-state electrical conductivity, magnetic moment, and spectrophotometric molar ratio and conductometric methods. The design and synthesis of a new bidentate ligand derived from 1,3-diphenyl-2,4-bis(3-amino-9-methoxy-1-phenyl-3H-benzo[f]chromene-2-carbonitrile for use in square planar or tetrahedral molecular templates have been successfully demonstrated. The synthesis of the ligand and its complexes proved to be as straightforward

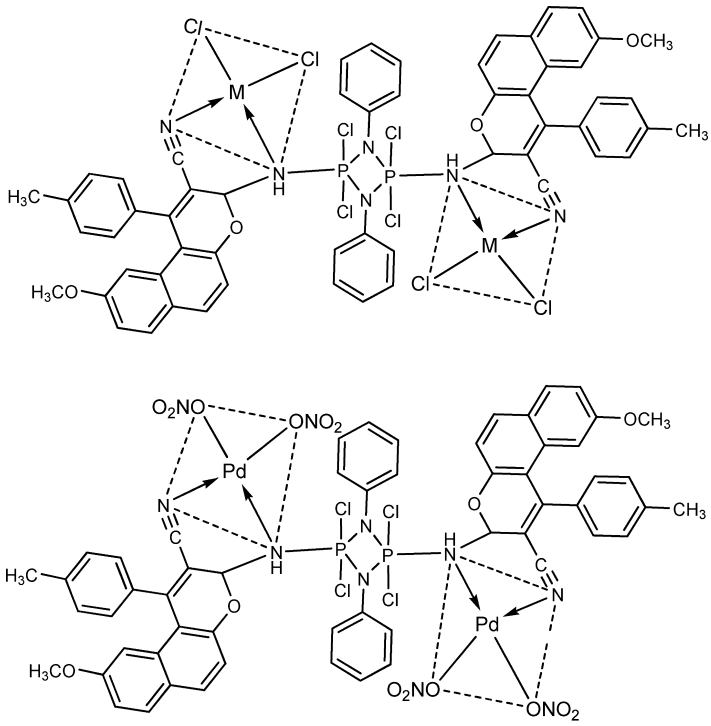

Where M = Co(II), Ni(II), and Cu(II)

SCHEME 2 Suggested structural formulae of **III** metal complexes.

as expected, giving high yields of the free ligand and its complexes in simple, one-pot reactions. As anticipated, the ligand coordinates equatorially to four-coordinate transition metal ions to give tetrahedral (Co(II), Ni(II)) and square planar (Cu(II), Pd(II)), environments around the metal ion anchor. The proposed general structures of the complexes are shown in Scheme 2. **III** ligand always coordinates *via* the imino-NH and carbonitrile-C≡N groups forming two-binding chelating sites.

EXPERIMENTAL

All chemicals used were of analytical reagent grade. They included $CoCl_2.6H_2O$, $NiCl_2.6H_2O$, $CuCl_2.2H_2O$, and $Pd(NO_3)_2$. $2H_2O$ and phosphorus pentachloride supplied from BDH. The solvents used were of analytical grade and were purified by standard

methods. The preparation of 3-amino-9-methoxy-1-phenyl-3H-benzo[f]-chromene-2-carbonitrile (II) was carried out according to the method in the literature.[33] 1,3-Diphenyl-2,2,2,4,4,4,-hexachlorocyclodiphosph-(V)azane (**I**) was prepared and purified using the method previously reported.[1,2]

Synthesis of Ligand

The solid of 3-amino-9-methoxy-1-tolyl-3H-benzo[f]chromene-2-carbonitrile (**II**) (3.28 g, 0.01 mmol) was added in small portions to a well-stirred solution of the 1,3-diphenyl-2,2,4,4-tetrachlorocyclodiphosph(V)azane (I) (3.79 g, 0.005 mmol) in acetonitrile (100 mL) over 30 min. After the complete addition, the reaction mixture was heated under reflux for 2 h with continuous stirring. After completion of the reaction (HCl gas ceased to evolve), the reaction mixture was filtered while hot and the filtrate was left to cool at room temperature. The obtained solid (yellow) was filtered, washed several times with acetonitrile, and dried *in vacuo* to give the corresponding 1,3-diphenyl-2,4-bis(3-amino-9-methoxy-1-tolyl-3H-benzo[f]chromene-2-carbonitrile)-2,2,4,4-tetrachlorocyclodiphosph(V)azane (**III**) (Scheme 1). Yield 90.0%, ^{1}H-NMR (300MHz; DMSO-d_6): 7.28–7.56 (32H, m, J = 8.1 Hz, Ar-H); 3.90 (6H s, J = 4.7 Hz, 2OMe); 8.97 (2H br, s, NH). ^{13}C-NMR (300MHz; DMSO-d_6): 154.11, 152.26, 151.30, 149.14, 148.31, 147.37, 146.53, 145.26, 144.32, 142.44, 141.37, 140.41, 137.83, 137.34, 136.99, 13.82, 129.63, 129.26, 128.97, 127.93, 127.76, 126.63, 122.52, 118.38 (all aromatic C) 158.27, 156.87 (2C≡N). ^{31}P-NMR (365 MHz; DMSO-d_6): 25.4 (phosphazo ring).

Synthesis of Complexes

A hot solution (60°C) of the metal salts ($CoCl_2$.$4H_2O$ [0.4 g; 0.002 mol]), ($NiCl_2$.$4H_2O$ [0.41 g; 0.002 mol]), ($CuCl_2$.$2H_2O$ [0.33 g; 0.002 mol]) or ($Pd(NO_3)_2$.$2H_2O$ [0.43 g; 0.002 mol]) in acetonitrile (50 mL) was added drop-wise to a hot solution of 1,3-diphenyl-2,4-bis(3-amino-9-methoxy-1-tolyl-3H-benzo[f]chromene-2-carbonitrile)-2,2,4,4-tetrachlorocyclodiphosph(V)azane (**III**) (0.658 g; 0.001 mol) in acetonitrile (100 mL) in a 2:1 metal-to-ligand molar ratio at room temperature with continuous stirring. After complete addition of the hot metal-salt solution, the reaction mixture was heated under reflux for about 2 h under dry conditions. The complexes obtained were washed with acetonitrile and then with dry diethyl ether and dried *in vacuo*.

Apparatus and Experimental Conditions

Elemental Analysis and Metal Percentage

Elemental analyses (C, H, N, Cl, and S) were performed using a Perkin-Elmer CHN 2400 elemental analyzer. Percentages of the metal ions of the complexes were determined using PYEUNICAM SP 1900 atomic absorption spectrophotometer supplied with the corresponding lamp used for this purpose. The phosphorus content was determined gravimetrically as phosphoammonium molybdate.[34]

IR Spectra

The KBr infrared spectra were recorded on Perkin-Elmer 1430 IR spectrophotometer covering the frequency range 200–4000 cm^{-1}. Calibration of the frequency readings was made with polystyrene film.

UV-Vis Spectra

The spectral studies were measured using a PYE-Unicam spectrophotometer model 1750 covering the wavelength range 190–900 mm. The complexes were measured in nujol mull following the method described by Lee et al.[35]

^{1}H, ^{13}C, and ^{31}P NMR Spectra

^{1}H and ^{13}C NMR spectra were recorded in $(CD_3)_2SO$ on a Varian Gemini 200 MHz or on a Varian Mercury 300 MHz Em-360-60 MHz spectrometer at Cairo University and shifts were expressed in δ units using TMS as internal reference. ^{31}P NMR spectra were run, relative to external H_3PO_4 (85%), with a Varian FT-80 spectrometer at 36.5 MHz.

Magnetic Susceptibility Measurements

Molar magnetic susceptibility corrected for diamagnetic using Pascal's constant was determined at room temperature (298 K) using Faraday's method. The apparatus was calibrated with Hg [Co(SCN)4].[36]

X-Ray Powder Diffraction

The X-ray powder diffraction analyses were carried out by using Rigku Model ROTAFLEX Ru-200. Radiation was provided by copper target (Cu anode 2000 W) high-intensity X-ray tube operated at 40 kV and 35 MA. Divergence slit and the receiving slit were 1 and 0.1, respectively.

Electrical Conductivity

Conductivity measurements were made on discs having 1 mm thickness of 1,3-diphenyl-2,4-bis(3-amino-9-methoxy-1-tolyl-3H-benzo[f]

chromene-2-carbonitrile)-2,2,4,4-tetrachlorocyclodiphosph(V)azane (**III**) and its complexes sandwiched between two copper electrodes. The conductivity cell used was the same as that reported in the literature.[37] The electrical conductivity was measured in the temperature range 30–150°C. The activation energies were calculated using the equation $\sigma = \sigma^{\circ} \exp(-E/2\,kT)$.

Thermal Analysis

Thermogravimetric analysis was performed under a nitrogen atmosphere using a Shimadzu TGA-50H with a flow rate of 20 mL min^{-1}.

ESR Spectra

ESR spectra were recorded at 100 kHz modulation and 10 G modulation amplitude on a Varian E-9 Spectrophotometer. Incident power of 10 mV was used and resonance conditions were at ca 9.75 GHz (X-band) at room temperature. Spectra were obtained with an air products LTD-3-110 Heli-Trans liquid helium transfer refrigerator. The field was calibrated with a powder sample of 2,2-diphenyl pyridylhydrazone (DPPH) $g = 2.0037$.[38]

Antimicrobial Activity

Antimicrobial activity was performed using DMF as solvent at Fermentation Biotechnology and Applied Microbiology (FERM-BAM) Center, Al-Azhar University, Egypt. The test was done using a diffusion agar technique.

REFERENCES

[1] A. M. A. Alaghaz and M. M. El-Desoky, *Al-Azhar Bull. Sci.*, **17,** 1 (2006).
[2] A. M. A. Alaghaz and S. A. H. Elbohy, *Phosphorus, Sulfur, and Silicon*, **183,** 2012–2031 (2008).
[3] E. H. M. Ibrahim, I. M. Abd-Ellah, L. S. Showki, and I. Alaimi, *Phosphorus, Sulfur, and Silicon*, **33,** 109 (1987).
[4] A. M. A. Alaghaz, PhD thesis, Faculty of Science, Al-Azhar University (Boys), Cairo, Egypt, 2004.
[5] A. N. Al-Khazandar, R. S. Farag, and I. M. Abd-Ellah, *Proc. Indian Natl. Sci. Acad.*, **60A,** 793 (1994).
[6] I. M. Abd-Ellah, E. H. M. Ibrahim, and A. N. Al-Khazandar, *Phosphorus, Sulfur, and Silicon*, **13,** 13 (1987).
[7] I. M. Abd-Ellah, Y. Al-Shaibi, A. A. Ba-issa, and M. S. El-Hammadi, *Phosphorus, Sulfur, and Silicon*, **139,** 29 (1998).
[8] J. V. Pustinger, W. T. Cove, and M. L. Neilsen, *Spectrochim. Acta*, **15,** 909 (1959).
[9] D. E. C. Corbridge, *J. Appl. Chem.*, **6,** 456 (1956).
[10] L. C. Thomas and R. A. Chittenden, *Chem. Ind. London*, **18,** 1913 (1961).
[11] A. M. A. Alaghaz and H. A. Gumaa, *Al-Azhar Bull. Sci.*, **17,** 73 (2006).
[12] R. B. Harvey and J. E. Mayhood, *Can. J. Chem.*, **33,** 1552 (1955).

[13] L. C. Scheinman, *Introduction to Spectroscopic Methods for the Identification of Organic Compounds*, 1st ed. (Elsevier, London, 1970) p. 173.
[14] J. H. Aupers, Z. H. Chohan, N. M. Comerlato, R. A. Howi, A. C. Silvino, J. L. Wardell, and S. M. S. V. Wardell, *Polyhedron*, **21,** 2107 (2002).
[15] S. E. Wiberley, S. C. Bunce, and W. H. Bauer, *Anal. Chem.*, **32,** 217 (1960).
[16] M. Becke-Goehring and B. Z. Bopple, *Anorg. Chem.*, **322,** 239 (1963).
[17] K. Nakamoto, *Infrared and Raman Spectra of Inorganic and Coordination Compounds* (Wiley, New York, 1978).
[18] G. J. Kleywegt, W. G. R. Wiesmeijer, G. J. V. Driel, W. L. Driessen, J. Reedijk, and J. H. Noordik, *J. Chem. Soc., Dalton Trans.*, 2177 (1985).
[19] I. M. Abd-Ellah, B. A. El-Sayed, M. A. El-Nawawy, and A. M. A. Alaghaz, *Phosphorus, Sulfur, and Silicon*, **177,** 2895 (2002).
[20] K. I. Goldberg, J. V. Martinez, G. E. Perez, L. A. Ackerman, and D. X. West, *Polyhedron*, **18,** 1177 (1999).
[21] N. F. Mott, and E. A. Davis, *Electronic Processes in Non-Crystalline Materials* (Clarendon Press, Oxford, 1971).
[22] D. F. Shriver, P. W. Atkins, and C. H. Langford, *Inorganic Chemistry* (Oxford University, Oxford, 1996).
[23] D.A. Seanor, *Electrical Properties of Polymers* (Academic Press, New York, 1982).
[24] B. D. Cullity, *Elements of X-ray Diffraction*, 2nd ed. (Addison-Wesley, New York, 1993).
[25] A. Bencini and D. Gattechi, *EPR of Exchange Coupled Systems* (Springer-Verlag, Berlin, 1990).
[26] B. K. Singh, R. K. Sharma, and B. S. Garg, *J. Therm. Anal. Catal.*, **84,** 593 (2006).
[27] A. W. Coats and J. P. Redfern, *Nature*, **68,** 201 (1964).
[28] B. K. Singh, R. K. Sharma, and B. S. Garg, *Spectrochim. Acta A*, **63,** 96 (2006).
[29] M. A. Ibrahim, A. A. H. Ali, and F. M. Maher, *J. Chem. Tech. Biotechnol.*, **55,** 217 (1992).
[30] I. M. Abd-Ellah, M. E. Hussein, A. N. El-Khazandar, and R. S. Farag, *Orient. Chem.*, **7,** 121 (1991).
[31] A. S. A. Zidan, *Phosphorus, Sulfur, and Silicon*, **178,** 567 (2003).
[32] A. Chaudhary and R. V. Singh, *Phosphorus, Sulfur, and Silicon*, **178,** 603 (2003).
[33] A. M. El-Agrody, F. A. Eid, H. A. Emam, H. M. Mohamed, and A. H. Bedair, *Z. Naturforsch.*, **57b,** 579–585 (2002).
[34] R. Voy, *Chem. Ztg. Chem. Apparatus*, **21,** 441 (1897).
[35] P. H. Lee, E. Griswold, and J. Kleinberg, *Inorg. Chem.*, **3,** 1278 (1964).
[36] N. B. Figgs and J. Lewis, *Modern Coordination Chemistry* (Interscience, New York, 1967), p. 403.
[37] M. A. Ahmed and F. A. Radwan, *J. Phys. Chem. Solid.*, **49,** 1385 (1988).
[38] D. Reinen and G. Friebel, *Inorg. Chem.*, **23,** 791 (1984).